



Faculty of Electronic and Computer Engineering



Abdullah Mohammed Saghir Zobilah

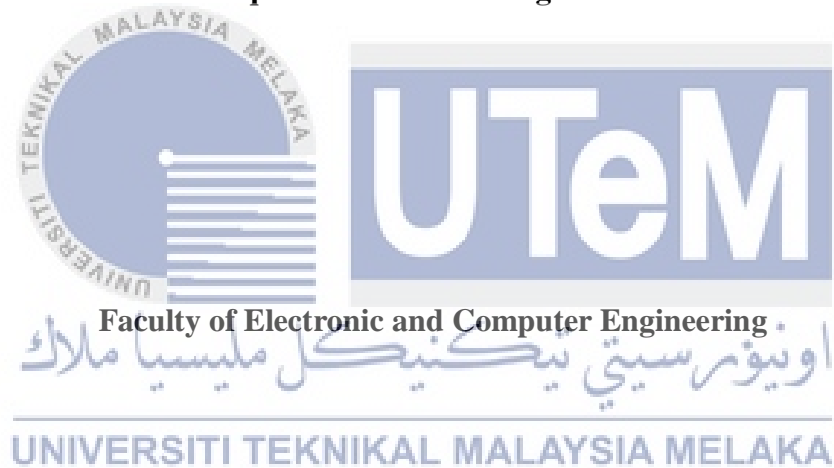
Doctor of Philosophy

2021

**DESIGN OF ABSORPTIVE FILTER INTEGRATED SWITCH USING LOSSY
RESONATORS AT 2.4 GHz ISM BAND**

ABDULLAH MOHAMMED SAGHIR ZOBILAH

**A thesis submitted
in fulfillment of the requirements for the degree of Doctor of Philosophy**



UNIVERSITI TEKNIKAL MALAYSIA MELAKA

2021

DECLARATION

I declare that this thesis entitled “Design of Absorptive Filter Integrated Switch using Lossy Resonators at 2.4 GHz ISM Band” is the result of my own research except as cited in the references. The thesis has not been accepted for any degree and is not concurrently submitted in candidature of any other degree.



Signature

Name



: Abdullah Mohammed Saghir Zobilah

Date

29 November 2021

اونيوورسيٲى ٲيٲنيكل مليا ملاك

UNIVERSITI TEKNIKAL MALAYSIA MELAKA

APPROVAL

I hereby declare that I have read this thesis and in my opinion this thesis is sufficient in terms of scope and quality for the award of Doctor of Philosophy.

	Signature	:	
	Supervisor Name	:	Dr. Noor Azwan Bin Shairi
	Date	:	29 November 2021

اونيورسيتي تيكنيكل مليسيا ملاك
UNIVERSITI TEKNIKAL MALAYSIA MELAKA

DEDICATION

To my beloved mother and father



ABSTRACT

Radio frequency (RF) and microwave switches are important components in RF front end, as they control the signal circulation path. Up to now, many different types of RF and microwave switches have been designed. They usually have a very wide passband with no specific band selectivity. With the increasingly complex spectrum environment and the increased communication modes, the traditional design method has the drawback of large circuit size, high impedance matching loss, and high fabrication cost. Researchers have recently become interested in a microwave switch with integrated filtering response, which has the potential to solve these issues. Thus, several research works have been done to develop a filter integrated switch (FIS). Based on the literature, most of the previous studies introduced reflective FISs having a problem of extremely low reflection coefficient at the ports that are not switched to the antenna or called OFF-state ports. In this research work, a reconfigurable resonator-based absorptive filter integrated switch (FIS) was presented for the industrial, scientific, and medical (ISM) band. Three types of reconfigurable resonators were utilized (L-shape, ring, and T-shape resonator). The FIS was made up of two absorptive resonators, reconfiguring between band-stop and band-pass responses, and integrated with a single pole double throw (SPDT) switch. In particular, the FIS circuit was designed for the purpose of switching between the transmitter (Tx) mode and the receiver (Rx) mode, as well as to filter both the transmitted and received signals. A simple mathematical analysis of isolation and insertion loss of filter integrated SPDT switch was discussed. PIN diodes were used as the switching elements for the SPDT switch and to reconfigure between the band-stop and band-pass responses. The band-stop response was the ultimate reason for the isolation between the transmitter (Tx) and receiver (Rx). While the bandpass response was the ultimate reason for selecting the wanted signal. The proposed absorptive FIS design could be used for ISM band applications at an operation frequency of 2.45 GHz. As a result, the proposed FIS design exhibited 2 dB of insertion loss and better than 38 dB of isolation. The measurement results showed a good agreement with the simulation results. Therefore, the key advantages of the proposed FIS design include low insertion loss, high isolation and good reflection coefficient at both ON- and OFF-state ports. In addition, the proposed FIS has an absorptive feature with a smaller number of PIN diodes while maintaining a compact size.

REKA BENTUK SUIS BERSEPADU PENAPIS PENYERAP MENGGUNAKAN PENYALUN HILANG PADA JALUR ISM 2.4 GHz

ABSTRAK

Suis frekuensi radio (RF) dan gelombang mikro adalah komponen penting di bahagian depan RF untuk mengawal peredaran isyarat. Sehingga kini, banyak jenis suis RF dan gelombang mikro telah direka bentuk. Suis-suis ini biasanya mempunyai ciri jalur-lepas yang sangat luas tetapi tiada pemilihan jalur tertentu. Melihat kepada persekitaran frekuensi spektrum yang semakin kompleks dan mod komunikasi yang semakin meningkat, kaedah reka bentuk tradisional mempunyai kekurangan dari segi saiz litar yang besar, kehilangan padanan yang tinggi, dan peningkatan kos pembuatan. Para penyelidik baru-baru ini telah berfokus kepada suis gelombang mikro dengan penapis bersepadu, yang berpotensi untuk menyelesaikan masalah-masalah ini. Oleh itu, beberapa kerja penyelidikan telah dilakukan untuk suis bersepadu penapis (FIS). Berdasarkan literatur, kebanyakan penyelidikan terdahulu telah memperkenalkan FIS reflektif yang mempunyai masalah pekali pantulan yang sangat rendah di liang yang tidak beralih ke antena atau dipanggil liang berkeadaan tertutup. Suis bersepadu penapis berpenyerap yang berasaskan resonator yang dapat dikonfigurasi dilaporkan dalam tesis penyelidikan ini untuk jalur industri, saintifik, dan perubatan (ISM). Tiga jenis resonator yang dapat dikonfigurasi telah dipilih iaitu bentuk L, cincin, dan bentuk T. FIS ini terdiri daripada dua resonator berpenyerap, konfigurasi antara sambutan jalur-henti dan jalur-lepas, dan disatukan dengan suis satu kutub dua lontar (SPDT). Secara khusus, litar FIS ini dirancang untuk tujuan pensuisan antara mod pemancar (Tx) dan mod penerima (Rx), serta untuk menyaring isyarat yang dihantar dan yang diterima. Satu analisis mudah matematik untuk pemencilan dan kehilangan sisipan SPDT bersepadu penapis telah dibincangkan. Diod-diod PIN digunakan sebagai elemen peralihan untuk SPDT dan untuk mengkonfigurasi antara sambutan jalur-henti dan jalur-lepas. Sambutan jalur-henti adalah ciri utama prestasi pemencilan antara pemancar (Tx) dan penerima (Rx). Manakala, sambutan jalur-lepas adalah sebab utama untuk memilih isyarat yang dikehendaki dan menghalang isyarat gangguan. Reka bentuk FIS berpenyerap yang dicadangkan ini dapat digunakan untuk aplikasi jalur ISM pada frekuensi 2.45 GHz. Hasilnya, FIS yang dicadangkan menghasilkan kehilangan sisipan sebanyak 2 dB dan pemencilan yang melebihi 38 dB. Hasil pengukuran menunjukkan persamaan yang hampir dengan hasil simulasi. Oleh itu, kelebihan utama reka bentuk FIS yang dicadangkan ini adalah kehilangan penyisipan yang rendah, pemencilan tinggi dan pekali pantulan yang baik di kedua-dua liang berkeadaan terbuka dan tertutup. Selain itu, FIS berpenyerap ini mempunyai bilangan diod PIN yang sedikit disamping mengekalkan saiz litar yang padat.

ACKNOWLEDGMENTS

I would like to thank my supervisor Dr. Noor Azwan Bin Shairi from Faculty of Electronic and Computer Engineering, Universiti Teknikal Malaysia Melaka (UTeM) for his essential supervision, support and encouragement to accomplish this thesis. The door to Dr. Noor Azwan Bin Shairi was always open whenever I had a question about my research or writing. He steered me in the right direction whenever he thought I needed it.

I also would like to thank my co-supervisor Prof. Dr. Zahriladha Bin Zakaria for his advice, recommendations and suggestions throughout this project.

Thanks to all my colleagues, my beloved mother, father, wife and siblings for their moral support in completing this degree. Finally, thanks to everyone who motivated me to finish up my project.



TABLE OF CONTENTS

	PAGE
DECLARATION	i
APPROVAL	ii
DEDICATION	iii
ABSTRACT	i
ABSTRAK	ii
ACKNOWLEDGMENTS	iii
TABLE OF CONTENTS	iv
LIST OF TABLES	vii
LIST OF FIGURES	viii
LIST OF APPENDICES	xx
LIST OF ABBREVIATION	xxi
LIST OF SYMBOLS	xxii
LIST OF PUBLICATIONS	xxiii
SCHOLARSHIPS	xxv
CHAPTER	1
1. INTRODUCTION	1
1.1 Introduction	1
1.2 Problem Statement	3
1.3 The Objectives	4
1.4 Scope of Work	5
1.5 Contribution of the Thesis	6
1.6 Thesis Organization	6
2. LITERATURE REVIEW	9
2.1 RF Switch	9
2.1.1 RF Switch Elements and Performance	9
2.1.2 Applications of RF Switch	11
2.1.3 Configurations of RF Switch	12
2.1.4 Operation of RF Switch	13
2.1.5 SPDT Switch	14
2.2 Absorptive Feature	29
2.2.1 Absorptive Band-stop Filters	29
2.2.2 Reconfigurable Absorptive Filters	35
2.2.3 Switchable Absorptive Filters	39
2.2.4 Absorptive RF Switch	42
2.2.5 Integrated RF Designs	48
2.3 Absorptive Band-Stop Filter Using Lossy Resonator	51
2.3.1 Realization	56
2.3.2 Tuneable Filter	57
2.4 Recent Progress on Filter integrated Switch (FIS)	65
2.5 Summary	89

3.	RESEARCH METHODOLOGY	90
3.1	Introduction	90
3.2	Flow Chart of the Project	90
3.3	The Specifications of Absorptive Filter-integrated SPDT Switch	92
3.4	Mathematical Modeling	92
3.4.1	Conventional Series PIN Diode Switch	92
3.4.2	Stub Resonator	94
3.4.3	Matched Lossy Resonators	95
3.5	The Absorptive Filter-Integrated SPDT Switch	95
3.5.1	The Absorptive Filter-Integrated SPDT Switch Using L-Shape Resonator	96
3.5.2	The Absorptive Filter-Integrated SPDT Switch Using Ring Resonator (R-FIS)	105
3.5.3	The Absorptive Filter-Integrated SPDT Switch Using T-Shape Resonator	113
3.6	Simulation and Layout	121
3.7	Fabrication, Soldering and Measurement	124
3.7.1	Soldering Process	126
3.7.2	Measurement Process	127
3.8	Summary	127
4.	RESULTS AND DISCUSSION	128
4.1	Introduction	128
4.2	Mathematical Modelling	128
4.2.1	The Isolation of Filter-Integrated SPDT Switch	129
4.2.2	The Insertion Loss of Filter-Integrated SPDT Switch	130
4.3	The Absorptive Filter Integrated Switch Using L-Shape Resonator	133
4.3.1	Parametric Study	133
4.3.2	The Result of L-Shape Switchable Resonator	137
4.3.3	The Result of The Absorptive Filter Integrated SPDT Switch	139
4.4	The Absorptive Filter Integrated Switch Using Ring Resonator	142
4.4.1	Parametric Study	142
4.4.2	The Result of Ring Switchable Resonator	147
4.4.3	The Result of The Absorptive Filter Integrated SPDT Switch	149
4.5	The Absorptive Filter Integrated Switch Using T-Shape Resonator	152
4.5.1	Parametric Study	152
4.5.2	The Result of T-shape Switchable Resonator	154
4.5.3	The Result of The Absorptive Filter Integrated SPDT Switch Using T-Shape Resonator	157
4.6	Comparison Between the Switchable Resonator Designs	159
4.7	Comparison between the FIS Designs	163
4.8	Comparison Between the Proposed FIS and The Previous Studies	166
4.9	Summary	168
5.	CONCLUSION AND FUTURE WORK	170
5.1	Conclusion	170
5.2	Suggestion for Future Work	172

REFERENCES
APPENDICES

173
190



LIST OF TABLES

TABLE	TITLE	PAGE
2.1	Summary of some absorptive RF devices	48
2.2	Summary of the filter-integrated switch research works	86
2.3	Comparison between this work and the related studies	89
3.1	The Specifications of Absorptive Filter-integrated SPDT Switch	92
3.2	Summary of Rx and Tx operation for (L-FIS)	105
3.3	Summary of Rx and Tx operation for (R-FIS)	113
3.4	The process summarization of the absorptive ring FIS	121
3.5	FR-4 Specification	122
4.1	The simulation result of the L-SR	138
4.2	The simulation and measurement results of the L-FIS	142
4.3	The simulation result of the R-SR	149
4.4	The simulation and measurement results of the R-FIS	151
4.5	The simulation result of the T-SR	156
4.6	The simulation and measurement results of the T-FIS	159
4.7	Comparison between this work and the related studies	168

LIST OF FIGURES

FIGURE	TITLE	PAGE
1.1	RF front-end system with SPDT switch	1
1.2	The diagram of the (a) conventional filter and SPDT switch, (b) filter integrated SPDT switch (Zhang, Xu and Chen, 2017)	2
2.1	Diagram of (a) DPDT switch (b) SPDT switch in RF-front end	12
2.2	Basic RF switch configuration, (a) series RF switch (b) shunt RF switch (c) series-shunt RF switch (Berezniak and Korotkov, 2013)	13
2.3	RF front-end system with SPDT switch	15
2.4	Photograph of the broadband SPDT switch (Zhao et al., 2017)	16
2.5	Simulated (dotted curves) and measured (solid curves) results of the broadband SPDT switch (Zhao et al., 2017)	16
2.6	Micrograph of the proposed SPDT switch (Shu and Gu, 2017)	17
2.7	Simulated (dashed line) and measured (solid line with symbol) results	17
2.8	Layout of the SPDT switch (Esfeh et al., 2018)	18
2.9	The result of (a) insertion loss, (b) isolation of the SPDT switch	19
2.10	Microphotograph of the fabricated SPDT-LNA (Ju et al., 2016)	20
2.11	Simulated (dashed) and measured (solid) S-parameters of the SPDT in transmit mode (Ju et al., 2016)	20
2.12	The prototype of the SPDT switch (Hojo and Ishizaki, 2015)	21
2.13	Simulated result of the proposed SPDT switch (Hojo and Ishizaki, 2015)	21

2.14	The diagram of the SPDT switch (Guo et al., 2016)	22
2.15	The simulation results of the isolation and Insertion loss	22
2.16	The prototype of the SPDT-2 (Osmanoglu and Ozbay, 2019)	23
2.17	Comparison result of the insertion loss and isolation of the three switches (Osmanoglu and Ozbay, 2019)	23
2.18	The prototype of the SPDT switch (Peng and Zhao, 2019)	24
2.19	The measurement and simulation of the insertion loss and reflection coefficient of the SPDT switch (Peng and Zhao, 2019)	24
2.20	The photograph of the proposed SPDT (Gong et al., 2019)	25
2.21	Simulated and measured (a) insertion loss and reflection coefficient (b) isolation	26
2.22	The photographs of the SPDT switches: (a) series SPDT switch (b) series-shunt SPDT switch (Lee and Hong, 2018)	27
2.23	Measurement and simulation results of the isolation and reflection coefficient at off-port (Lee and Hong, 2018)	27
2.24	The layout of SPDT switch (Akmal et al., 2018)	28
2.25	The Simulated results of the SPDT switch (Akmal et al., 2018)	28
2.26	(a) The prototype of the absorptive band-stop filter (b) the microstrip circuit model (Shao and Lin, 2014)	30
2.27	Simulated result of the absorptive filter (Shao and Lin, 2014)	30
2.28	The (a) Prototype, and (b) circuit diagram of the absorptive filter using lossy resonator (Shao and Lin, 2015)	31
2.29	Simulation result of the absorptive filter using lossy resonator	31
2.30	The diagram of the absorptive band-stop filter (Stander et al., 2014)	32
2.31	The prototype of fabricated absorptive band-stop filter	33

2.32	The simulation and measurement results, isolation (S_{12}) and reflection coefficient (S_{11}) (Psychogiou et al. 2015)	33
2.33	Topology of the proposed ABSF (Liu et al., 2017)	34
2.34	Measured and simulated results of the proposed 3-stage ABSF	34
2.35	Circuit configuration of proposed narrowband BABSF	35
2.36	Simulated and measured results of proposed BABSF for a Differential mode (Kong et al., 2018)	35
2.37	The circuit diagram during (a) band-stop operation, (b) bandpass operation (Lee et al., 2020)	36
2.38	The result during (a) band-stop mode, (b) bandpass mode	36
2.39	The (a) 3D diagram of the filter structure, and (b) isolation and reflection coefficient of the absorptive filter (Snow et al., 2012)	37
2.40	Filter diagram (Naglich et al., 2014)	38
2.41	Measurement and simulation result (Naglich et al., 2014)	38
2.42	The diagram of the reconfigurable filter (Guyette et al., 2016)	39
2.43	Measurement of the proposed filter (Guyette et al., 2016)	39
2.44	Prototype of reconfigurable bandstop to all pass filter	40
2.45	Simulated (m2) and measured (m1) result (a) absorptive bandstop response (b) all-pass response (Zahari et al., 2012)	40
2.46	Photo of the fabricated switchable filter (Allen et al., 2018)	41
2.47	The response of the switchable bandpass to absorptive band-stop filter	42
2.48	The (a) circuit diagram of the absorptive SPDT switch, and (b) measured result of the switch (Yang and Yang, 2013)	42
2.49	The diagram of the absorptive SPDT switch (Fang et al., 2017)	43
2.50	The reflection coefficient during Off-state (Fang et al., 2017)	43

2.51	The Fabricated SPST switch (Semnani et al., 2018)	44
2.52	Comparison of the simulated and measured results of the SPST switch	44
2.53	The diagram of the proposed methodology (Wei and Negra, 2018)	45
2.54	Measured and simulated isolation (Wei and Negra, 2018)	45
2.55	The diagram of the absorptive SPDT switch (Trinh et al., 2019)	46
2.56	The simulated and measured results of the absorptive SPDT switch	46
2.57	The diagram of the SP4T switch (Suh and Min, 2019)	47
2.58	The measurement and simulation result of the absorptive SP4T	48
2.59	The prototype of the LNA integrated with high-power RF switch	49
2.60	Noise figure and small-signal gain of LNA integrated with RF switch	49
2.61	The layout and picture of the design (Gómez-García et al., 2018)	50
2.62	The simulation and measurement of isolation (S_{21}), insertion loss (S_{31}) and reflection coefficient (S_{11}) (Gómez-García et al., 2018)	50
2.63	Distributed-element enhancement-Qu notch filter (Jachowski, 2004)	51
2.64	Absorptive band-stop filter circuit implementation (Guyette et. al., 2005)	52
2.65	Even-mode admittance of a lossy resonant circuit (Guyette et. al., 2005)	53
2.66	High Q absorptive band-stop response (Guyette et. al., 2005)	55
2.67	A coupled resonator model of absorptive band-stop filter	55
2.68	L-shape absorptive band-stop filter	56
2.69	First experimental realizations of the absorptive bandstop filter using lossy resonators in microstrip technology (a) L-shape (parallel coupled) resonator (b) Dual mode ring resonator (c) Folded ring resonator	57
2.70	Intrinsically switched tunable absorptive band-stop filter	58
2.71	Intrinsically switched tunable notch filter prototype simulated and measured results with bandwidth tuning (Guyette, 2012)	58

2.72	Prototype of tunable impedance inverter of matched notch filter	59
2.73	Tunable k-inverter of coupled $\lambda/4$ resonators (Wong et al., 2007)	59
2.74	Measured result of notch filter with bias (V_b) tuning from 2.2V to 4.2V for (a) transmission (b) reflection responses	60
2.75	The simulated and measured results of the filter. (a) S_{11} . (b) S_{21}	61
2.76	Prototype of the switchable bandpass to band-stop filter	61
2.77	Simulation and measurement results during bandpass response	62
2.78	Simulation and measurement results during band-stop response	62
2.79	(a) photo of the proposed multifunctional and reconfigurable filter, (b) part of the result of the multifunctional and reconfigurable filter	63
2.80	The prototype of the bandpass to band-stop (Kumar and Singh, 2017)	64
2.81	The simulated result of the filter (a) With transmission poles. (b) Without any TP on transmission poles (Kumar and Singh, 2017)	65
2.82	Conventional (a) filter and switch, (b) integrated filter and switch	65
2.83	5th-order SPST FIS (Lee et al., 2006)	66
2.84	Measurement during switch condition ON and OFF vs. frequency	66
2.85	3rd-order SPDT FIS (Chao et al. 2007)	67
2.86	S-parameters results when ON (port 2) and OFF (port 3)	67
2.87	1 GHz SPDT FIS (Tsai et al., 2007)	67
2.88	Frequency response comparison between conventional filter and hybrid SPDT switch at 1 GHz (Tsai et al., 2007)	67
2.89	60 GHz MMIC SPDT FIS (Tsai et al., 2007)	68
2.90	Isolation and reflection coefficient during OFF-state of switch (Tsai et al., 2007)	68
2.91	4th-order six port FIS (Chao et al., 2007)	68

2.92	Result at the isolation port when port 1 and 5 are ON-state	68
2.93	Reduced-sized SPDT FIS (Lee et al., 2008a)	69
2.94	Measurement and simulation of isolation (Lee et al., 2008a)	69
2.95	50 GHz reduced-sized SPDT FIS (Lee et al., 2008b)	70
2.96	Measurement and simulation of S-parameters (Lee et al., 2008b)	70
2.97	Filter-integrated PIN diode switch (Phudpong et al., 2009)	70
2.98	S-parameters at ON-state of Tx. (Phudpong et al., 2009)	70
2.99	Switchable BPF (Liao et al., 2010)	71
2.100	Filter response during OFF-state (Liao et al., 2010)	71
2.101	DPDT FIS (Chao and Shih, 2012)	72
2.102	Measurement result of DPDT FIS (Chao and Shih, 2012)	72
2.103	Absorptive bandpass FIS (Perhirin and Auffret, 2013)	72
2.104	Results of absorptive bandpass FIS during Tx ON state	72
2.105	Bandpass filter integrated to SPDT switch (Chao, 2012)	73
2.106	S-parameter results of SPDT FIS at thru port and isolated port (Chao, 2012)	73
2.107	SPST bandpass filter integrated switch (Lee and Nguyen, 2014)	74
2.108	S-parameter for SPST FIS (Lee and Nguyen, 2014)	74
2.109	3rd-order switchable SPDT bandpass filter (Chen et al., 2014)	75
2.110	Narrowband response of FIS (Chen et al., 2014)	75
2.111	SPDT bandpass FIS (Rave et al., 2014)	75
2.112	S-parameters for both ON and OFF states (Rave et al., 2014)	75
2.113	(a) S ₂₁ response for an integrated SP2T switch and filter with the switch in the off-state (O V), (b) S ₂₁ response for the left	

	switch and filter with the switch on (7 V) and with 10 VDC applied to the filter, and (c) S21 response for the right switch	76
2.114	(a) 3-D illustration of the proposed standing-wave filter integrated SPST switch. (b): Measured results of the proposed filter integrated SPST switch (Ma et al., 2013)	77
2.115	(a) Photograph of the implemented 60-GHz filtering SPDT. (b) Measured results of the switchable artificial-resonator-based standing wave SPDT filtering switch (Ma et al., 2013)	77
2.116	PCB photograph of proposed SPDT switchable BPF with single and differential outputs (Chen and Lin, 2015)	78
2.117	Measured and simulated responses when the SISO BPF path is switched on while the SIDO BPF path is switched off. (a) Narrowband $ S_{11} $, $ S_{41} $, and $ S_{44} $. (b) Wideband response and isolation performance (Chen and Lin, 2015)	78
2.118	Photograph of the proposed SISL SPDT switchable BPF	79
2.119	The simulated and measured responses of the proposed SISL SPDT switchable BPF (Li et al., 2016)	79
2.120	Photograph of fabricated quasi-elliptic bandpass filter-integrated SPDT switch (Ji et al., 2016)	80
2.121	Simulated and measured results of quasi-elliptic bandpass filter-integrated SPDT switch (Ji et al., 2016)	80
2.122	Simulated and measured results of fabricated filter-integrated SPDT switch (Xu et al., 2017)	81
2.123	The prototype of (a) DR SPST filtering switch (b) DR SPDT filtering switch (Zhang et al., 2017)	82

2.124	The measured and simulated result of filtering SPST switch (a) insertion loss and reflection coefficient (b) Isolation	83
2.125	The result of filtering SPDT switch (a) responses when filter 1 is ON and Filter 2 is OFF (b) responses when Filter 1 is OFF and Filter 2 is ONN (Zhang et al., 2017)	83
2.126	(a) The prototype of filtering SPDT switch (b) simulated and measured results (Xu et al., 2018)	84
2.127	Measured and simulation results of the T/R switch	85
3.1	The flow chart of the project	91
3.2	Diagram of single series SPDT switch using PIN diodes	92
3.3	(a) Single series connected PIN diode and (b) the equivalent circuit	93
3.4	The general diagram of open stub resonator	94
3.5	(a) A single parallel coupled line resonator, (b) the simulated frequency	97
3.6	(a) A double parallel coupled line resonator, (b) the simulated frequency	98
3.7	Matched lossy L-shape resonator and its parameters	99
3.8	Parametric study of (a) S_{12} and (b) S_{11} with variation in g_1	100
3.9	Parametric studies of (a) S_{12} and (b) S_{11} with variation in g_2	101
3.10	The diagram of the L-shape switchable resonator	103
3.11	Circuit diagram of the absorptive filter integrated SPDT switch using L-shape resonator (L-FIS)	105
3.12	Ring resonator and its parameters	106
3.13	Simulated frequency response of the ring resonator	107
3.14	The diagram of the switchable ring resonator	108
3.15	The simulated result of the switchable ring resonator during (a) band-stop and (b) bandpass response	108

3.16	Parametric studies of (a) S_{11} and (b) S_{12} during bandpass response of the ring resonator with variation in l_4	109
3.17	The switchable ring resonator	111
3.18	Circuit diagram of the absorptive filter integrated SPDT switch using ring resonator (R-FIS)	113
3.19	T-shape resonator	114
3.20	Simulated frequency response of the T-shape resonator	115
3.21	The effect of the microstrip line (l_1) on the performance of the T-shape resonator (a) reflection coefficient (S_{11}) (b) attenuation (S_{12})	116
3.22	The effect of the coupling gap (S) on the performance of the T-shape resonator (a) reflection coefficient (S_{11}) (b) attenuation (S_{12})	117
3.23	(a) The diagram of the T-shape resonator, (b) the simulated frequency	118
3.24	The diagram of the T-shape switchable resonator	119
3.25	The diagram of the absorptive FIS using T-shape switchable resonator	121
3.26	Schematic window of ADS Software	122
3.27	The line calculation window from the ADS	123
3.28	The layout window	123
3.29	The layout of the L-FIS	124
3.30	The UV Exposure Machine	125
3.31	The Etching Machine	126
3.32	Soldering tools	126
3.33	Agilent network analyser and power supply with the device under test	127
4.1	The general diagram of the proposed absorptive filter integrated SPDT	129
4.2	The diagram of the L-shape switchable resonator	133

4.3	Comparison result of the switchable L-shape resonator using different length of the gap (g_1) during band-stop (a) reflection coefficient (S_{11}) (b) attenuation (S_{12}), and band-pass (c) reflection coefficient (S_{11}) (d) insertion loss (S_{12})	135
4.4	Comparison result of the switchable L-shape resonator using different length of the gap (g_2) during band-stop (a) reflection coefficient (S_{11}) (b) attenuation (S_{12}), and band-pass (c) reflection coefficient (S_{11}) (d) insertion loss (S_{12})	136
4.5	The layout of the L-shape switchable resonator	138
4.6	The simulation result of the L-shape single pole single throw (L-SPST); (a) Insertion loss (S_{12}) and the reflection coefficient (S_{11}); (b) attenuation (S_{12}) and the reflection coefficient (S_{11})	139
4.7	The prototype of the absorptive FIS	139
4.8	Simulation and measurement results of the proposed design with TLSR, (a) isolation (S_{12}) (b) reflection coefficient (S_{11}), (c) reflection coefficient (S_{22}) and (d) insertion loss (S_{13})	141
4.9	The switchable ring resonator	142
4.10	Comparison result of the switchable ring resonator using different length of the gap (S) during band-stop (a) reflection coefficient (S_{11}) (b) attenuation (S_{12}), and band-pass (c) reflection coefficient (S_{11}) (d) insertion loss (S_{12})	143
4.11	Comparison result of the switchable ring resonator using different length of the transmission line (l_4) during band-stop (a) reflection coefficient (S_{11}) (b) attenuation (S_{12}), and band-pass (c) reflection coefficient (S_{11}) (d) insertion loss (S_{12})	145

4.12	Comparison result of the switchable ring resonator using different length of the transmission line (l_5) during band-pass (a) reflection coefficient (S_{11}), (b) insertion loss (S_{12})	146
4.13	The layout of the ring switchable resonator	147
4.14	The simulation result of the ring single pole single throw (R-SPST); (a) Insertion loss (S_{12}) and the reflection coefficient (S_{11}); (b) attenuation (S_{12}) and the reflection coefficient (S_{11})	148
4.15	The fabricated ring FIS	149
4.16	Simulation and measurement results of absorptive filter integrated SPDT switch, (a) isolation (S_{12}) (b) reflection coefficient (S_{11}) (c) reflection coefficient (S_{22}) (d) insertion loss (S_{13})	150
4.17	The diagram of the T-shape switchable resonator	152
4.18	Comparison result of the switchable T-shape resonator using different length of the gap (S) during band-stop (a) reflection coefficient (S_{11}) (b) attenuation (S_{12}), and band-pass (c) reflection coefficient (S_{11}) (d) insertion loss (S_{12})	154
4.19	The layout of the T-shape switchable resonator	154
4.20	The simulation result of the attenuation (S_{12}) and reflection coefficient of the T-shape switchable resonator (T-SR) during band-stop response	155
4.21	The simulation result of the insertion loss (S_{12}) and reflection coefficient of the T-shape switchable resonator (T-SR) during bandpass response	156
4.22	The prototype of the absorptive FIS using T-shape resonator	157
4.23	Simulation and measurement results of absorptive filter integrated SPDT switch using T-shape resonator, (a) isolation (S_{12}) (b) reflection coefficient (S_{11}) (c) reflection coefficient (S_{22}) (d) insertion loss (S_{13})	158

4.24	A comparison between the simulated insertion loss (S_{12}) during band-pass response of L-shape, ring and T-shape switchable resonators	160
4.25	A comparison between the simulated reflection coefficient (S_{11}) of band-pass response of L-shape, ring and T-shape switchable resonators	161
4.26	A comparison between the simulated attenuation (S_{12}) during band-stop response of L-shape, ring and T-shape switchable resonators	162
4.27	A comparison between the simulated reflection coefficient (S_{11}) during band-stop response of L-shape, ring and T-shape switchable resonators	163
4.28	A comparison between the simulated and measured isolation (S_{12}) of	164
4.29	A comparison between the simulated and measured reflection coefficient (S_{11}) of L-shape, ring and T-shape FISs	164
4.30	A comparison between the simulated and measured reflection coefficient OFF-port (S_{22}) of L-shape, ring and T-shape FISs	165
4.31	A comparison between the simulated and measured insertion loss (S_{13})	166

اوتیور سیتی تیکنیکل ملیسیا ملاک

UNIVERSITI TEKNIKAL MALAYSIA MELAKA